THE REGULATION OF TRANSMEMBRANE METALLOPROTEINASES AND THEIR FUNCTIONS

by

Congyu Lu

A thesis submitted to the Faculty of the University of Delaware in partial fulfillment of the requirements for the degree of Master of Science in Biological Sciences

Summer 2018

THE REGULATION OF TRANSMEMBRANE METALLOPROTEINASES AND THEIR FUNCTIONS

by

Congyu Lu

Approved: _____
Shuo Wei, Ph.D.
Professor in charge of thesis on behalf of the Advisory Committee

Approved: _____
E. Fidelma Boyd, Ph.D.
Chair of the Department of Biological Sciences

Approved: _____
George H. Watson, Ph.D.
Dean of the College of Arts and Sciences

Approved: _____
Douglas J. Doren, Ph.D.
Interim Vice Provost for Graduate and Professional Education

ACKNOWLEDGMENTS

I would like to thank my advisor, Dr. Shuo Wei, for his invaluable support and guidance during my studies. He is not only a good advisor, but also a good friend. He always helps and encourages me during my difficult times.

I am very grateful to Dr. Erica Selva and Dr. Deni Galileo for serving on my committee and helping me throughout my degree. Their expertise and advices are greatly appreciated.

I would also like to thank all the present and past members of the Wei laboratory for their guidance and support. Thank you to all my friends for the fun and support in the past two years.

Lastly, I want to thank my fiancée and my family for always being there for me.

TABLE OF CONTENTS

LIST OF TABLES

LIST OF FIGURES

ABSTRACT

Members of the metzincin superfamily of metalloproteinases, including the disintegrin and metalloproteinases (ADAMs) and the matrix metalloproteinases (MMPs), have long been associated with diseases such as cancer and arthritis. Among all the metzincin metalloproteinases, transmembrane metzincins such as transmembrane ADAMs and transmembrane MMPs, have emerged as new targets for cancer therapy. In this study, I investigated the mechanisms of action and regulation of 3 transmembrane metalloproteinases that have been implicated in tumor progression (ADAM9, ADAM12 and MMP14), to better understand the roles they play in cancer and provide guidance for targeting them as novel approaches of cancer treatment.

Previous research in our lab suggests that ADAM9, which is highly expressed in many types of solid tumors, promotes colorectal cancer (CRC) progression. To understand the mechanism of action for ADAM9, I carried out RNA-seq in HCT116 human CRC cells with ADAM9 knockdown. A total of 351 differentially expressed genes (DEGs), including 93 up-regulated genes and 258 down-regulated genes, were identified. My enrichment analysis revealed that MAPK signaling pathway, p53 signaling pathway and FoxO signaling pathway, are significantly enriched. These pathways may mediate the function of ADAM9 in CRC progression.

My bioinformatics analysis predicts the C-terminal lysine residue in the cytoplasmic tail of several ADAMs may be ubiquitinated to target these ADAMs for proteasome-mediated degradation. One of these ADAMs, ADAM12, has been implicated in the pathology of malignant tumors, such as breast cancer. To test if the C-terminal K903 residue is important for ADAM12 turnover, I generated the K903R mutant, as well as a mutant with the whole cytoplasmic tail deleted. I found that the

levels of both mutants are elevated as compared with wild-type ADAM12. My findings indicate that the most C-terminal lysine residue of ADAM12 is likely involved in its degradation.

The third part of this research concerns a cross-regulation of transmembrane metalloproteinases by cysteine proteases. We found that treatment of both normal and neuroblastoma cells with K777, a cysteine protease inhibitor, leads to post-transcriptional accumulation of MMP14. Surprisingly, MMP14 substrates also accumulate in the cells, suggesting that the activity of this transmembrane MMP is actually inhibited. We therefore hypothesize that the accumulation of MMP14 upon K777 treatment is due to reduced autocleavage. Consistent with this hypothesis, a protease-dead mutant of MMP14 does not accumulate after K777 treatment. These results unveil a possible crosstalk between cysteine proteases and transmembrane metalloproteinases, which warrants further investigation.

Chapter 1

BACKGROUND

The metzincin superfamily of metalloproteinases is generally characterized by an HEXGHXXGXXH zinc binding motif at the active site and a conserved methionine residue within the catalytic domain [1-2]. Based on the composition of domains and subtle differences in the catalytic site, the metzincin superfamily can be further divided into various subfamilies such as Matrix metalloproteinases (MMPs), a disintegrin and metalloproteinases (ADAMs), and a disintegrin and metalloproteinase with thrombospondin motifs (ADAMTSs) [3]. The metzincin superfamily of metalloproteinases is mainly involved in the proteolysis of proteins at cell surface and proteins in the extracellular matrix (ECM), regulating cell–ECM and cell–cell interactions [4]. Metzincins have long been associated with cancer progression [5]; among all the metzincin metalloproteinases, transmembrane metzincins such as transmembrane ADAMs and membrane-type MMPs, have emerged as new targets for cancer therapy [6-7].

ADAM metalloproteinases typically have a cytoplasmic tail, a transmembrane domain, and an extracellular region that is composed of a pro domain, a metalloproteinase domain, a disintegrin-like domain, a cysteine rich domain, and an epidermal growth factor (EGF)-like domain [8]. ADAM metalloproteinases are synthesized as zymogens, which have a pro domain to inhibit their protease activity. To activate the ADAM metalloproteinases, the pro domain of ADAMs has to be removed by proprotein convertases, such as furin, to unmask the catalytic site [9].

Proteolytically active ADAMs are capable of cleaving various substrates such as growth factors, cytokines, and a wide variety of receptors [10]. Recently, multiple members of ADAMs, including ADAM9, ADAM10, ADAM12, ADAM15 and ADAM17, have been shown to play a role in cancer [7].

Matrix metalloproteinases (MMPs), also known as matrixins, are one class of metzincins that are primarily secreted metalloproteinases [11]. Among the 25 known MMPs, six MMPs are targeted to the cell surface and are called membrane-type MMPs (MT-MMPs). MT-MMPs can be further divided into transmembrane MMPs (MMP14, MMP15, MMP16 and MMP24) and glycosyl phosphatidylinositol (GPI)-anchored MMPs (MMP17 and MMP25) [12]. The transmembrane MMPs have a propeptide, followed by a metalloproteinase domain, a hinge region, a hemopexin domain, a stalk region, a transmembrane domain, and a cytoplasmic tail [12]. Like ADAM metalloproteinases, transmembrane MMPs are synthesized as zymogens, which have a propeptide to inhibit their protease activity and can be activated by the removal of pro domain [13-14]. Transmembrane MMPs mainly involved in cleaving ECM and cell surface proteins; among the 4 transmembrane MMPs, MMP14 has the widest substrate specificity [15]. Transmembrane MMPs have been shown to be associated with various cancers [6, 15]. For example, MMP14 was reported to promote cell invasion and migration in nasopharyngeal carcinoma [17] and enhance tumour growth and invasion in hepatocellular carcinoma [18]. A higher level of MMP15 was found in human lung adenocarcinoma and human breast cancer tissues [19-20]. MMP16 was also shown to promote tumor metastasis in hepatocellular carcinoma [21].

Transmembrane metalloproteinases have emerged as new targets for cancer therapy [6-7]. In this study, I investigated the mechanisms of action and regulation of 3 transmembrane metalloproteinases, to better understand the roles they play in cancer and provide guidance for targeting them as novel approaches of cancer treatment.

Chapter 2

RNA-SEQ REVEALS TRANSCRIPTOME CHANGES IN COLORECTAL CANCER CELLS FOLLOWING ADAM9 KNOCKDOWN

2.1 Introduction

Colorectal cancer (CRC) is one of the most aggressive human cancers and is the third most common malignancies in the United States. Symptoms of colorectal cancer include constipation, diarrhea, rectal bleeding, unexplained weight loss, abdominal bloating, anemia, and jaundice [22-23]. Every year, there are about 160,000 new cases of colorectal cancer and 57,000 deaths from the disease in the United States [24]. The five-year survival rate is 90% for colorectal cancer found at the localized stage and 71% for colorectal cancer found at the regional stage. If the cancer has spread to distant parts of the body (distant stage), the 5-year survival rate drops to 14% [24-25]. There is an urgent need to understand the molecular mechanisms of colorectal cancer progression in order to develop more effective therapeutic strategies.

Colorectal cancer originates from the epithelial cells lining the colon or rectum of the gastrointestinal tract, and aberrant activation of Wnt signaling pathway is responsible for oncogenesis of over 80% of colorectal cancer [26-27]. The canonical Wnt pathway, also known as the Wnt/β-catenin pathway, has an important role in carcinogenesis and is essential for cancer stem cell maintenance [28]. In the Wnt/β-catenin pathway, the extracellular Wnt ligand binds with its cell surface receptor, which through intracellular signaling protects the cytosolic protein β-catenin from degradation. This increase in β-catenin allows it to translocate into the nucleus to act as a transcriptional coactivator and initiate transcription of target genes [29].

ADAM family proteins belong to the metzincins superfamily of metalloproteinases and function in shedding diverse cell surface receptors and

signaling proteins [30]. They not only play important roles in the regulation of cell-cell signaling during development and homeostasis, but also are involved in tumor formation and progression. Among all the ADAM proteins, ADAM9 has crucial functions in various types of cancers. High ADAM9 expression has been reported in many types of cancers, including breast, lung, brain and bladder cancers. Expression level correlates well with tumor progression in some cancers [31-32]. ADAM9 is thus a new potential biomarker for diagnosis and drug target for the treatment of cancer. In our previous research, we found that knockdown of ADAM9 does not only reduce the canonical Wnt signaling, but also reduces cancer cell migration in colorectal cancer cells [33]. However, the underlying mechanism of how ADAM9 regulates colorectal cancer remains elusive. Here I use an RNA-Seq approach to comprehensively investigate the differentially expressed genes in ADAM9-knockdown colorectal cancer cells. I also conduct enrichment analysis to further determine the role of ADAM9 in the regulation of colorectal cancer. This comprehensive analysis helps identify the transcriptomic changes in the ADAM9-knockdown colorectal cancer cells and improve our understanding of the molecular mechanisms through which ADAM9 regulates colorectal cancer.

2.2 Materials and Methods

2.2.1 Cell Culture and Transfection

Colorectal cancer cell line HCT116, which has a high ADAM9 expression, was purchased from ATCC and cultured in McCoy's 5A medium (ATCC) containing 10% fetal bovine serum (FBS) and Pen-Strep (100 U/mL Penicilium and 100 μg/mL Streptomycin) in 5% CO_2 at 37°C. Cells were grown to 40% confluence and

transfected with ADAM9 siRNA using Lipofectamine 3000 (Invitrogen). The medium was refreshed 12 h after transfection, and the cells were further incubated for another 48 h.

2.2.2 RNA Isolation and Quality Control

Total RNA was extracted from ADAM9-knockdown cells and control cells using RNeasy Mini Kit (QIAGEN, USA) according to the manufacturer's instructions. Quality of the RNA was estimated using the A260:A280 ratio and RNA degradation and contamination were monitored by electrophoresis in 1% agarose gels. Integrity and size distribution of RNA was evaluated using a Bioanalyzer. The total RNA samples were treated with DNase I to degrade DNA contamination.

2.2.3 RNA-Seq Library Preparation and Sequencing

Illumina RNA-Seq library construction and sequencing was conducted by the University of Delaware DNA Sequencing & Genotyping Center (Newark, DE). Six replicates of each treatment were subject to RNAseq and high throughput sequencing was completed using the Illumina HiSeq 2500 system (Illumina).

2.2.4 Quality Control, Trimming and Filtering Reads

After obtaining the RNA-Seq Raw data in the FASTQ format, the quality of the raw data was evaluated with FastQC, which is a quality control tool for high throughput sequence data and provides a modular set of analyses that give a quick impression of whether the raw data has any potential abnormalities [34]. The low quality read ends and adapter sequences were removed and the low-quality reads were filtered out using Trim Galore, which is a wrapper tool around Cutadapt and FastQC for trimming and filtering Illumina data [35].

2.2.5 Reference Mapping and Feature Counting

After the trimming and filtering, all the reads were aligned to the hg19 human reference genome using TopHat2, which is built on the ultrafast short read mapping program Bowtie and is a popular choice for mapping reads to an annotated reference genome [36]. HTseq-count, a tool developed with HTSeq that preprocesses RNA-Seq data, was used to count how many reads map to each annotated genes [37].

2.2.6 Differential Gene Expression Analysis and Enrichment Analysis

The differential gene expression analysis was conducted using the R packages DEseq and edgeR, which provide statistical routines for determining differential expression in digital gene expression data using a model based on the negative binomial distribution [38-39]. False discovery rate (FDR) was used for multiple test correction and the exact test in edgeR was conducted to determine the differentially expressed genes (DEGs) between the ADAM9-knockdown and control colorectal cancer cells with a cutoff threshold of corrected p-value < 0.05 and fold change >1.5. Gene Ontology (GO) and pathway enrichment analysis of the DEGs were performed using Enrichr, which is an online tool for comprehensive enrichment analysis [40].

2.3 Results

2.3.1 Visualization of Sample-to-Sample Distances

To assess overall similarity between samples, the principal component analysis (PCA) plot and the multi-dimensional scaling (MDS) plot were created using EDseq and edgeR [38-39], respectively. As shown in Fig. 1 and Fig. 2, most sample variance is observed between control samples and ADAM9-knockdown samples. The control samples and the ADAM9-knockdown samples were separated in both the PCA plot

and the MDS plot. Also, the ADAM9-knockdown samples are more similar to each other compared to the control samples. Two of the control samples are not very similar to the rest of the control samples, however, since the 2 control samples were separated from the ADAM9-knockdown samples, the dissimilarity was considered as acceptable variance among control samples.

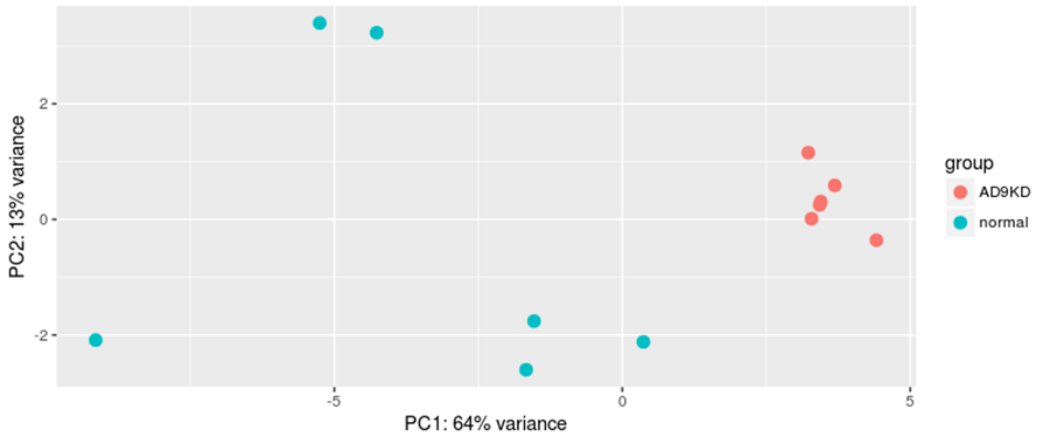

Figure 1: A PCA plot showing the sample-to-sample distances. The PCA plot uses linear algebra techniques to find the optimal rotation of the coordinate system so that most of the variation among samples is represented in 2 dimensions. Horizontal axis (PC1) captures 64% variance and vertical axis (PC2) captures 13% variance.

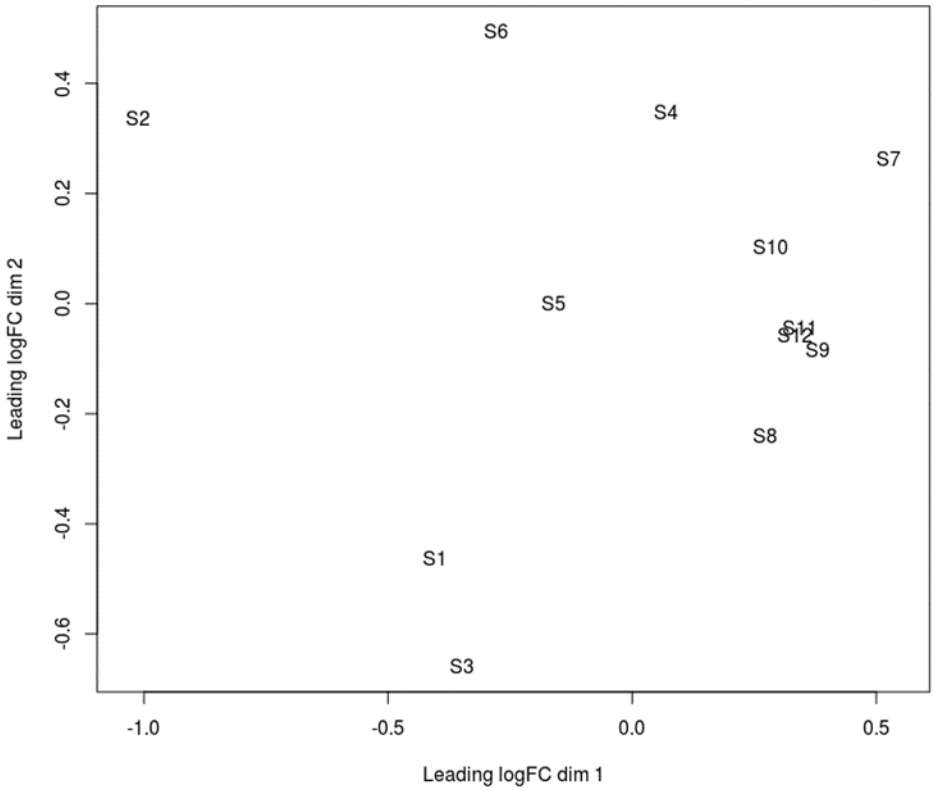

Figure 2: An MDS plot showing the sample-to-sample distances. The MDS plot maps the highly dimensional data for each sample into two dimensions. S1-S6 are 6 replicates of the control samples. S7- S12 are 6 replicates of the ADAM9-knockdown samples.

2.3.2 Identification of DEGs between ADAM9-Knockdown and Control Colorectal Cancer Cells

The dispersion, which is a measurement of the variability among biological replicates, was calculated using the edgeR estimateDisp function [38]. Then a BCV (biological coefficient of variation) plot was generated to show the relationship between the biological coefficient of variation for each gene and the mean log count per million (CPM) for that gene across all replicates. As shown in Fig. 3, BCV decreases to a steady lower level as counts of genes increase.

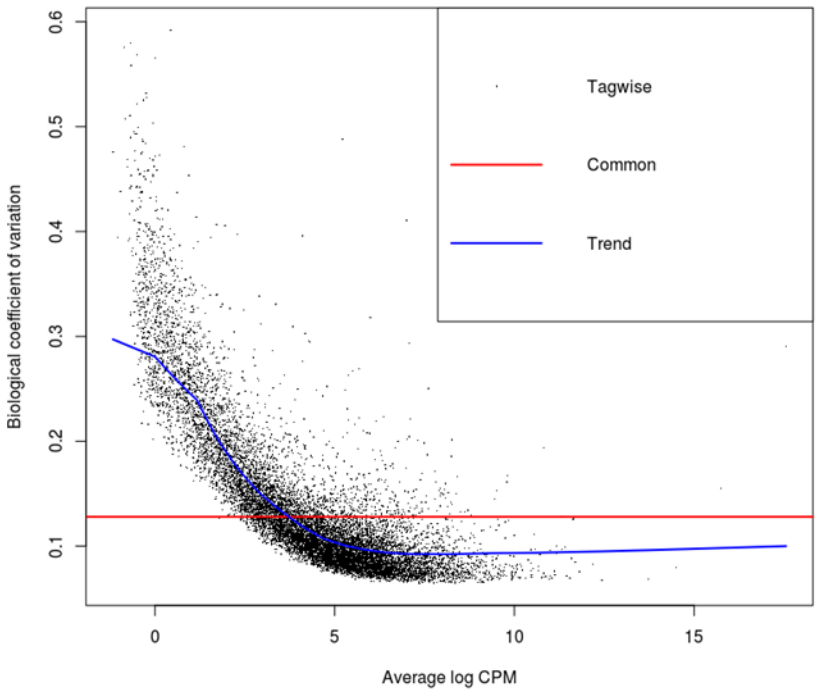

Figure 3: A BCV plot showing the relationship between the biological coefficient of variation and the average log CPM. The BCV plot shows the biological coefficient of variation (the square root of the dispersion) for each gene vs. the mean log CPM for that gene across all replicates. A black point is shown for each gene, with a blue curve indicating the trend and a red line showing the overall BCV across all genes.

The exact test in edgeR was conducted to determine the differentially expressed genes (DEGs) between the ADAM9-knockdown and control colorectal cancer cells with a cutoff threshold of corrected p-value < 0.05 and fold change >1.5. A total of 351 DEGs, 93 up-regulated genes and 258 down-regulated genes, were identified between the ADAM9-knockdown and control colorectal cancer cells. To visualize the differentially expressed genes, a plot of the log fold-change vs. the average log CPM was generated using plotSmear [38]. As shown in the Fig. 4, most of

the genes that meet the P-value threshold didn't pass the 1.5-fold change threshold, and most of the genes passed the 1.5-fold change threshold were down-regulated.

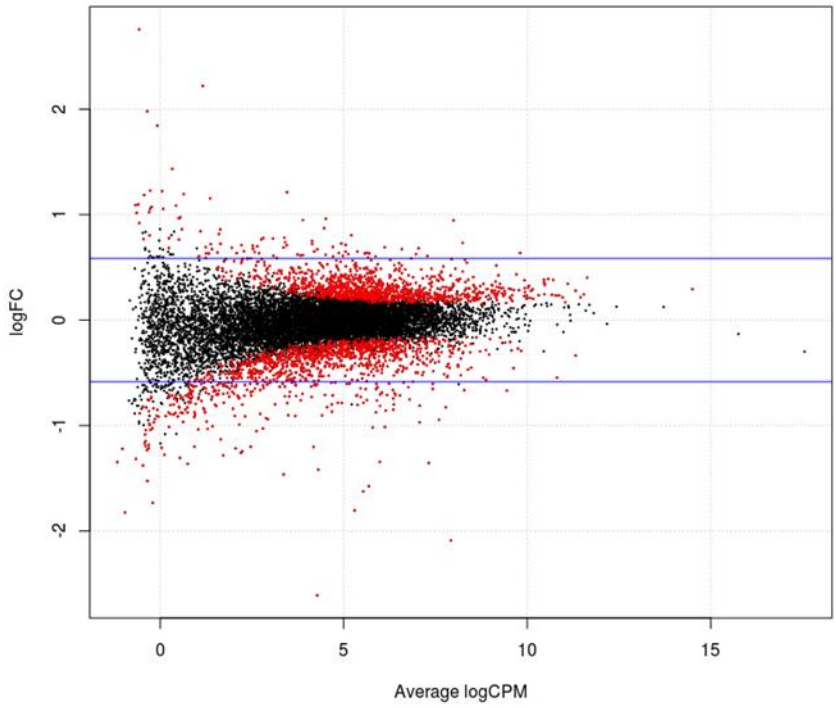

Figure 4: A plot of the log fold-change vs. the average log counts per million (CPM) showing the DEGs. DEGs whose expression is significantly altered ($P \leq 0.05$) are colored red, and the rest of the genes are colored black in the plot. The blue lines indicate fold-change of +/− 1.5-fold, respectively.

2.3.3 Enrichment Analysis of DEGs

The identified DEGs were further analyzed by Gene Ontology (GO) and pathway enrichment analysis using Enrichr [40]. As shown in Fig. 5, the top pathways that are significantly enriched by DEGs (P-values < 0.05) were identified by the KEGG pathway enrichment analysis. The pathway with the highest combined score is

the MAPK signaling pathway (p-value= 0.001917297) and it has extensive crosstalk with Wnt/β-catenin signaling in cancer [41-42]. The FoxO signaling pathway (p-value= 0.002436168), which has the second highest combined score, plays an important role in apoptosis and was shown to interact with β-catenin [43-44]. The pathway has the third highest combined score is the p53 signaling pathway (p-value= 0.007266505). Attenuated p53 pathway was observed in many patients with colorectal cancer and loss of p53 function has been shown to increase canonical Wnt signaling [25, 45].

The identified DEGs were also analyzed by Gene Ontology (GO) enrichment analysis. As shown in Fig. 6 and Fig. 7, the GO enrichment analysis identified many biological processes and molecular functions that are significantly enriched by DEGs (P-values < 0.05). A lot of biological processes and molecular functions identified are involved in amino acids transport and other transmembrane transporter activity, many genes encoding transmembrane transporters are the transcriptional target for p53 [46]. One of the biological process that has the highest combined scores is positive regulation of neuron apoptotic process, which is one of the major functions of p53 [47].

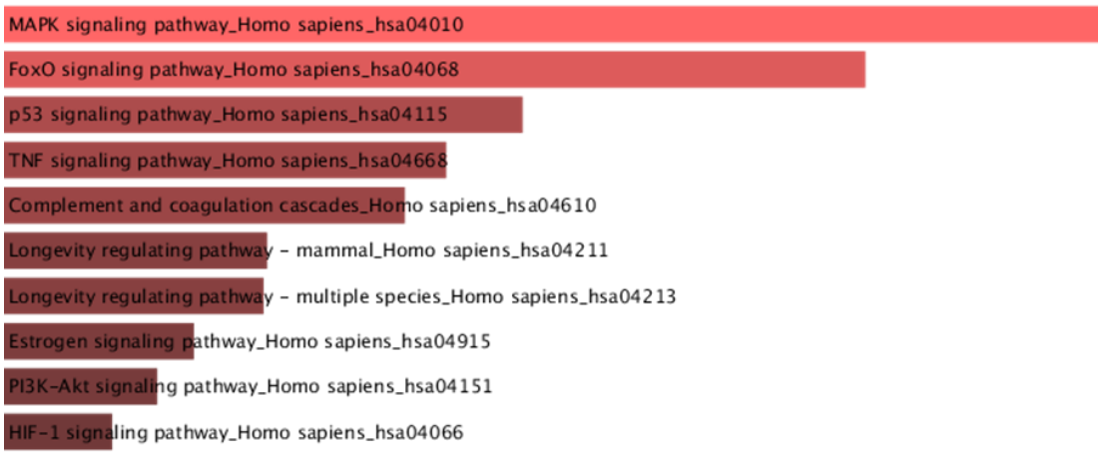

Figure 5: KEGG pathway enrichment analysis of the DEGs, sorted by combined score. The length of the bars represents the significance of that specific pathway.

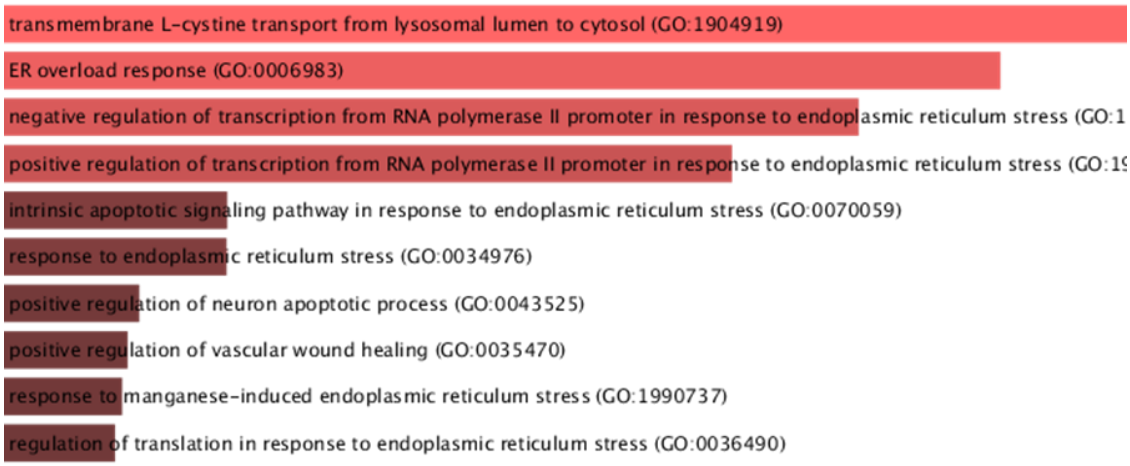

Figure 6: GO biological process enrichment analysis of the DEGs, sorted by combined score. The length of the bars represents the significance of that specific term.

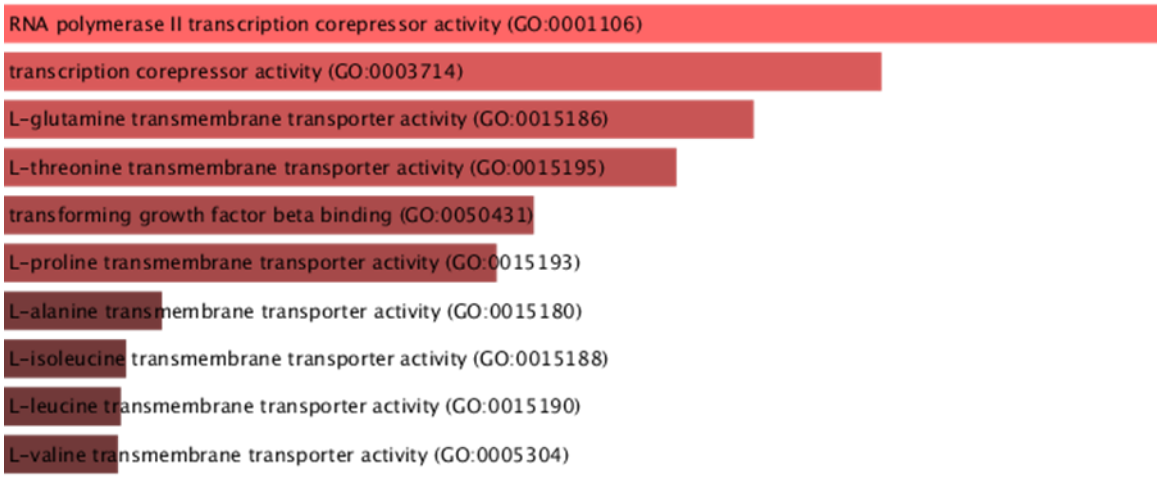

Figure 7: GO Molecular Function enrichment analysis of the DEGs, sorted by combined score. The length of the bars represents the significance of that specific term.

2.4 Conclusion

Recently, ADAM9 has emerged as a new potential biomarker for diagnosis and drug target for the treatment of cancer. In our previous research, we found that knockdown of ADAM9 does not only reduce the canonical Wnt signaling, but also reduces cancer cell migration in colorectal cancer cells [33]. However, the underlying mechanism of how ADAM9 regulates colorectal cancer remains elusive. In this study, I used an RNA-Seq approach to comprehensively investigate the differentially expressed genes between the ADAM9-knockdown and control colorectal cancer cells with a cutoff threshold of corrected p-value < 0.05 and fold change >1.5. A total of 351 DEGs, including 93 up-regulated genes and 258 down-regulated genes, were identified. My KEGG pathway enrichment analysis of the DEGs identified that MAPK signaling pathway, FoxO signaling pathway and p53 signaling pathway have the highest combined scores. The mitogen-activated MAPK signaling pathway has been shown to have extensive crosstalk with Wnt/β-catenin in cancer. Stimulation of

the Wnt/β-catenin pathway stabilize Ras and therefore activates the MAPK pathway [41-42]. The FoxO signaling pathway plays an important role in apoptosis and was shown to interact with β-catenin, which is one of the most important players in Wnt signaling pathway [43-44]. Attenuated p53 pathway was observed in many patients with colorectal cancer and loss of p53 function has been shown to increase canonical Wnt signaling [25, 45]. Also, many biological processes and molecular functions identified by my GO enrichment analysis are related to p53. The 3 significantly enriched pathways identified are all closely related to Wnt signaling pathway, indicating the important role of Wnt signaling pathway and its interaction with MAPK, p53 and FoxO signaling pathway play in the regulation of colorectal cancer cells by ADAM9.

Chapter 3

REGULATION OF ADAM12 TURNOVER

3.1 Introduction

ADAM12, initially called meltrin α, is a member of the ADAM (a disintegrin and metalloproteinase) protein family [48]. As a consequence of alternative splicing, there are two naturally occurring human ADAM12 splice variants, ADAM12-L and ADAM12-S. ADAM12-L, the membrane-bound form, is a type I transmembrane protein and it has a typical structure of the transmembrane metalloproteinases. ADAM12-L has a cytoplasmic tail, a transmembrane domain, and an extracellular region that is composed of a pro domain, a metalloproteinase domain, a disintegrin-like domain, a cysteine rich domain, and an epidermal growth factor (EGF)-like domain. ADAM12-S, on the other hand, is a secreted form of ADAM12 that is truncated. In ADAM12-S, the transmembrane domain and the cytoplasmic tail are replaced by a unique stretch of 33 amino acids [49-50].

ADAM12 is considered as an active metalloproteinase and has a number of substrates in the extracellular matrix or on the cell surface. ADAM12-L is believed to shed the ectodomain of many EGFR ligands including epidermal growth factor (EGF), heparin-binding EGF-like growth factor (HBEGF), and betacellulin (BTC), resulting in EGFR signaling [51-52]. EGFR signaling not only plays an important role in the regulation of cell proliferation, differentiation and migration, but also has been shown to be involved in the promotion of various cancers originating from epithelial tissues [53]. ADAM12-L was also shown to cleave Delta-like 1, a known mammalian Notch ligand, and activate Notch signaling [54]. Moreover, ADAM12-L has been suggested to cleave fibronectin, gelatin and type IV collagen in the extracellular matrix (ECM)

[55]. On the other hand, ADAM12-S was shown to cleave the insulin-like growth factor-binding proteins (IGFBP)-3 and IGFBP-5, releasing the IGFs and activating IGFR signaling [56-57].

ADAM12 has been implicated in several pathological processes including asthma, liver fibrogenesis, and hypertension [58-60]. Most of all, ADAM12 is remarkably upregulated in a variety of human tumors [61]. Some research demonstrated that ADAM12-L was specifically upregulated whereas others showed the increased expression of both the transmembrane and soluble forms of ADAM12 [62-65]. Studies have shown that in urine of breast cancer patients and bladder cancer patients, ADAM12 is increased and the levels of ADAM12-S present in the urine of patients correlates with breast and bladder cancer stage [57, 62]. There is also research showing that ADAM12-L is predominantly expressed in glioblastomas and its transcript level is considerably higher in the glioblastomas than in nonneoplastic brain tissues [66]. Another study demonstrated that ADAM12 mRNA levels are upregulated in liver cancer and mRNA levels of ADAM12 correlates with tumor aggressiveness and progression [63].

Due to the involvement of ADAM12 in a variety of pathological processes especially in various cancers, ADAM12 has emerged as a new and promising drug target. However, it is very difficult to use inhibitors to target the metalloproteinase domain with any specificity since there is high structural similarity between the ADAM12 and many other metalloproteinases [57, 61]. Therefore, a better understanding of the molecular mechanism that regulates ADAM12 level, such as turnover of ADAM12, may provide us novel means to control the activity of this metalloproteinase for therapeutic purposes.

In our previous research, we found that the most C-terminal lysine residue of ADAM13 is conserved among many species and is predicted to be ubiquitinated [67]. In *Xenopus*, we found that knockdown of ADAM19 causes ADAM13 degradation because ADAM19 binds with ADAM13 and protects it. However, ADAM13 won't be degraded in the absence of ADAM19 if its most C-terminal lysine residue is substituted with arginine [67]. Interestingly, the most C-terminal residue of mouse ADAM12 is also a lysine and is predicted to be an ubiquitination site, indicating a similar function as the most C-terminal lysine residue of ADAM13 [68]. In this research, I investigated the role the most C-terminal lysine residue plays in the process of ADAM12 degradation, to obtain a better understanding of the molecular mechanism that regulates ADAM12 level and gain insight into ADAM12 associated pathological processes.

3.2 Materials and Methods

3.2.1 Prediction of Ubiquitination Sites

The C-terminal sequences of ADAM12 were obtained from GenBank and were used as input for the prediction of the ubiquitination sites. BDM-PUB, an algorithm that can computational predict protein ubiquitination sites with bayesian discriminant method, was used to conduct the prediction [68]. The threshold used was 0.3 and any position with a prediction score larger than 0.3 is predicted to be ubiquitinated.

3.2.2 Construction of the ADAM12 K903R Mutant Plasmid

The construction of the ADAM12 K903R mutant plasmid was initiated by PCR amplification of full length wild-type mouse ADAM12 using the primers with

specific mutation in its sequence to enable the substitution of the most C-terminal lysine residue to arginine. The sequences of the primers are forward: 5'-AAA AAA ATC GAT ATG GCA GAG CGC CCG G-3' and reverse: 5'-GTG GTC GAC CAC CTG ATA TAG GCA TTG-3'. The PCR products were then digested by ClaI and SalI and sub-cloned into pCS2+ plasmid with myc_6 tag in C-terminal to monitor its expression. The wild-type (WT) mouse ADAM12 and a mouse ADAM12 mutant with the whole cytoplasmic tail deleted (ΔC) constructs were generated previously in our laboratory.

3.2.3 Cell Culture and Transfection

The human embryonic kidneys cell line HEK293T was obtained from American Type Culture Collection (ATCC) and the cells were grown in Dulbecco's Modified Eagle's Medium (DMEM) containing 10% fetal bovine serum (FBS) and Pen-Strep (100 U/mL Penicilium and 100 μg/mL Streptomycin) at 37℃ in a humidified atmosphere with 5% CO_2. The HEK293T cells were transfected in 6-well tissue culture plates with plasmids and incubated for 48 hours before collection.

3.2.4 Cell Lysis and Western Blotting

The transfected HEK293T cells were lysed in cell lysis buffer (Cell Signaling) and the concentration of the protein was determined using the Bicinchoninic acid (BCA) assay (Thermo Scientific) with bovine serum albumin (BSA) as standard. For the western blotting, same amount of protein was loaded on SDS–PAGE gels and then electrotransferred onto nitrocellulose membranes (Bio-Rad). After blocking for 1 hour with 5% BSA and incubating for 1 hour with anti-myc primary antibody (1:1000)

(Santa Cruz), signals were detected by peroxidase-conjugated secondary antibodies using chemiluminescence reaction (Bio-Rad). Beta-actin was used as the loading control.

3.3 Results and Discussion

3.3.1 Prediction of Ubiquitination Sites

The C-terminal sequences of ADAM12 were used as input to conduct the prediction of ubiquitination sites. The algorithm used was BDM-PUB and any lysine residue with a score larger than the threshold 0.3 is likely to be ubiquitinated [68]. As shown in Table 1, from *Xenopus* to human, the most C-terminal lysine residue is conservative among many species and has a score much higher than 0.3 in all the species listed, so the lysine residue is very likely to be ubiquitinated.

Table 1: The C-terminal lysine residue of ADAM 12 is a potential ubiquitination site.

Species	C-Terminal Sequence	Score
X. trop Adam12	PGPTKPPQRK	5.2
Anolis Adam12	HRSCNAAYKQ	4.7
Chick Adam12	RSSNATADVK	4.6
Mouse Adam12	PRPSHNAYIK	4.3
Human Adam12	PRSTHTAYIK	4.6

The C-terminal 10 residues of ADAM12 from indicated species are aligned, and the lysine residue at or near the C-terminus is underlined. Scores were calculated by DM-PUB algorithm (http://bdmpub.biocuckoo.org) and scores above threshold (0.3 or higher) indicate high probability of ubiquitination.

3.3.2 Construction of the ADAM12 K903R Mutant Plasmid

The ADAM12 K903R mutant plasmid was constructed by amplifying the cDNA encoding wild-type mouse ADAM12 using the primers with specific mutation in its sequence to enable the substitution of the most C-terminal lysine residue to arginine, and then inserting the ADAM12 K903R sequence into the pCS2+ vector with myc_6 tag in its C-terminal. Diagnostic restriction digest was used to confirm the rough structure of the ADAM12 K903R mutant plasmid (Fig. 8) and the sequence of the ADAM12 K903R mutant was further verified by Sanger sequencing.

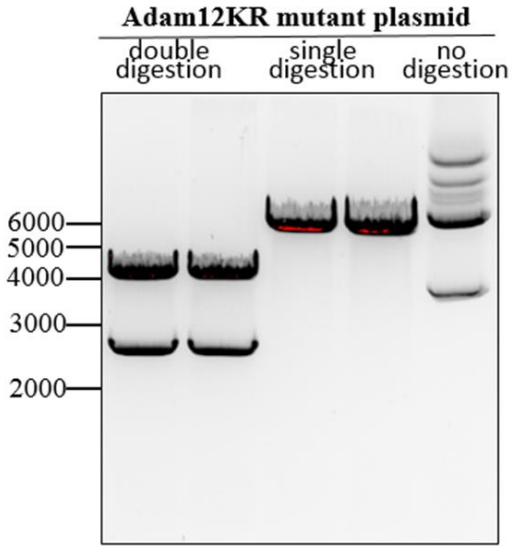

Figure 8: Diagnostic restriction digest of the ADAM12 K903R mutant plasmid. ADAM12KR mutant plasmid was digested by ClaI and SalI (double digestion), or ClaI only (single digestion), at 37 ℃ for 3 hours. Unit for the size is base pair.

3.3.3 Western Blotting

For the western blotting, anti-myc was used as the primary antibody to determine the level of wild-type mouse ADAM12 and its two mutants. As shown in

Fig. 9, the expression level of ADAM12 K903R mutant is much higher than wild-type ADAM12. The fact that substitution of the most C-terminal lysine by arginine stabilizes mouse ADAM12, combined with the result of the ubiquitination site prediction, indicates that the most C-terminal lysine residue of mouse ADAM12 is involved in its degradation by proteasome. Also, the level of an ADAM12 mutant with the whole cytoplasmic tail deleted (the ΔC mutant) is even higher than ADAM12 K903R mutant, suggesting that the lysine residue is not the only ubiquitination site in the cytoplasmic tail of mouse ADAM12.

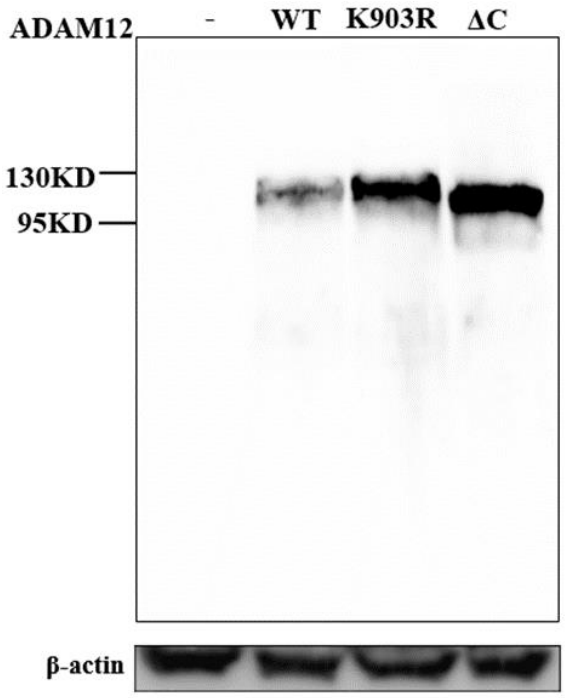

Figure 9: Substitution of the most C-terminal lysine by arginine stabilizes mouse ADAM12. HEK293T cells were transfected with 1 μg of plasmid encoding C-terminal myc_6-tagged wild-type ADAM12 (WT), the K903R mutant, or the ΔC mutant. Cell lysates were processed for western blot with an anti-myc antibody.

3.4 Conclusion and Future Directions

As an active metalloproteinase that has multiple substrates in the extracellular matrix or on the cell surface, ADAM12 has been implicated in many pathological processes especially in various human tumors [58-61]. As a result, it has emerged as a new and promising drug target. However, due to the high structural similarity between ADAM12 and many other metalloproteinases, it is very difficult to use inhibitors to target the metalloproteinase domain with any specificity. Therefore, a better understanding of the molecular mechanism that regulates ADAM12 level may provide us a novel mean to control the activity of this metalloproteinase for therapeutic purposes. In this study, I investigated the role of the most C-terminal lysine residue in the process of ADAM12 degradation. I found that the most C-terminal lysine residue of mouse ADAM12 is conserved among many species and is predicted to be ubiquitinated by the BDM-PUB algorithm [68]. I then constructed an ADAM12 K903R mutant plasmid and transfected the HEK293T cells with the plasmid along with wild-type mouse ADAM12 and the ΔC mutant. Their levels were compared using western blotting, and the result showed that the level of ADAM12 K903R mutant is much higher than the level of wild-type ADAM12, meanwhile, the level of the ΔC mutant is even higher than the ADAM12 K903R mutant. Overall, my study indicates that the most C-terminal lysine residue of mouse ADAM12 is involved in its degradation by proteasome and the lysine residue is not the only ubiquitination site in the C-terminal of mouse ADAM12. My findings provide new information for better understanding of the molecular mechanism regulates mouse ADAM12 degradation.

Future research that studies the binding between ADAM12 constructs and ubiquitin would be helpful to further understand the degradation mechanism of mouse ADAM12. Also, in our previous research, we found that ADAM19 binds with

ADAM13 and non-proteolytically protects it from degradation in vivo [67]. A similar mechanism of ADAM12 protection is expected, and studies investigating the interactions between ADAM12 and other ADAM family proteins are needed to better understand the process.

Chapter 4

THE REGULATION OF MMP14 IN K777-TREATED NEUROBLASTOMA CELLS

4.1 Introduction

Neuroblastoma is the most common solid tumor of childhood and the leading cause of cancer deaths in children under five [69]. About 800 new cases of neuroblastoma are diagnosed each year in the United States and approximately 90% of the cases are diagnosed by age 5 [69-70]. Neuroblastoma derives from the embryonic sympathoadrenal lineage of the neural crest and is often present as stage 3 or 4 in patients older than 2 year of age [71]. For these patients, aggressive treatments such as chemotherapy and radiation are typically used to eradicate the cancer. However, side effects of the aggressive treatments are particularly severe for children, and the 5-year survival rates for patients in stage 3 or 4 is below 50% [72-74]. Hence, there is an urgent need to develop more effective therapeutic strategies to treat this devastating disease.

Cathepsins, which are a group of lysosomal proteinases, play a significant role in a range of physiological and pathological processes such as lysosomal protein recycling, bone remodeling, prohormone and proenzyme activation, tumor progression and metastasis, rheumatoid arthritis, osteoarthritis and atherosclerosis [75-78]. The cathepsin family in humans contains 2 aspartic proteases (cathepsin D and E), 2 serine proteases (cathepsins A and G), and 11 cysteine cathepsins (cathepsins B, C, F, H, K, L, O, S, V, X and W) [76-77]. Among all the cathepsins, elevated levels of cathepsins B and L have been observed in several human cancers [79-85]. Evidence has shown that the levels of Cathepsins B and L increase in breast and prostate cancer and their levels correlate well with the invasiveness of breast and prostate cancer [80-82].

Furthermore, significantly higher expression of cathepsins B and L was also found in invasive types of histomorphologically benign meningioma, and the level of cathepsins B could be of critical value in the diagnosis of histomorphologically benign but invasive meningiomas tumors [83]. There are also studies showing that the levels of cathepsins B and L are remarkably higher in glioblastomas than in nonneoplastic brain tissues [84-85].

Due to their involvement in various tumors, cathepsins B and L are thought to represent two potential targets for tumor therapy [79]. K11777 (N-methyl-piperazine-Phe-homoPhe-vinylsulfone-phenyl), also known as K777, is a potent, irreversible cysteine protease inhibitor, and its targets include cathepsins B and L [86]. K777 was originally developed to target cruzain as a novel treatment for Chagas disease, a tropical disease caused by the protozoan parasite *Trypanosoma cruzi*, and it was shown to be safe and effective in preclinical mice and dog models of *T. cruzi* infection [87-89]. Recently, our collaborator Dr. Robert Mason at Nemours Alfred I. duPont Hospital for Children found that K777 treatment can specifically cause neuroblastoma cell death in vitro [90]. They also performed a proteomics analysis to identify the differentially expressed proteins between control and K777-treated neuroblastoma cells. Interestingly, matrix metalloproteinase-14 (MMP14), as well as various substrates of MMP14, were found to be upregulated in K777-treated neuroblastoma cells.

As a transmembrane MMP, MMP14 has a cytoplasmic tail, a transmembrane domain, and an extracellular region that is composed of a propeptide, a metalloproteinase domain, a hinge region, a hemopexin domain, and a stalk region [91-92]. MMP14 is synthesized and secreted to the cell surface in its pro-form, which

has a propeptide that blocks its active site and inhibits its protease activity. After the propeptide is removed, MMP14 will be in its active form and able to cleave a variety of proteins in the extracellular matrix or at the cell surface [91]. MMP14 is known to cleave collagen I to III, fibronectin, gelatin, fibrin, proteoglycans, and many other proteins in the extracellular matrix [91, 93]. At the cell surface, MMP14 was shown to form a trimolecular complex with pro-MMP2 and TIMP2 (tissue inhibitor of metalloproteinases-2), resulting in the activation of pro-MMP2 [94-95]. Moreover, there are also reports showing that MMP14 is capable of degrading itself through autocleavage [96-97].

The fact that many substrates of MMP14 were shown to be upregulated in K777-treated neuroblastoma cells indicates decreased activity of MMP14. However, a significantly higher level of MMP14 was also found in K777-treated neuroblastoma cells [90]. Since the main form of MMP14 that accumulates in K777-treated neuroblastoma cells is unknown, one possible explanation of the apparent contradiction between higher level of MMP14 and higher level of MMP14 substrates in K777-treated neuroblastoma cells is that K777 inhibits cathepsins B and L, and prevents the activation of MMP14 from its pro-form. The inhibition of MMP14 activation prevents MMP14 from cleaving its substrates and itself, causing the accumulation of pro-form of MMP14 and its substrates in K777-treated neuroblastoma cells.

MMP14-mediated cleavages of several substrates, such as type I collagen and EphA2, are critical for tumor progression [93-94]. In this research, I investigated the expression and activity of MMP14 in K777-treated cells, to obtain a better understanding of the molecular mechanism regulates MMP14 under K777 treatment

and provide more information for targeting cathepsins B and L as a novel approach to treat neuroblastoma.

4.2 Materials and Methods

4.2.1 Plasmids

The constructs of wild-type mouse MMP14 (WT MMP14; C-terminally myc_6-tagged), a protease-dead mutant (MMP14 E/A; C-terminally myc_6-tagged), and *Xenopus laevis* EphA2 (C-terminally HA-tagged) were generated previously in our laboratory. The mouse PTK7 construct (C-terminally HA-tagged) was a gift from Dr. Xiaowei Lu at University of Virginia. All plasmids were verified by Sanger sequencing (University of Delaware DNA Sequencing & Genotyping Center).

4.2.2 Cell Culture and Transfection

Cell culture was conducted as described in section 3.2.3. The HEK293T cells were transfected in 6-well tissue culture plates with 3 ADAM12 plasmids and incubated for 48-72 hours before collection.

4.2.3 K777 Treatment

K777 was a gift from Dr. James Mckerrow at UCSD and was dissolved in DMSO at a concentration of 10 mM. After transfection, cells were treated with 10 μM K777 and incubated for 48-72 hours before collection. 10 μM DMSO was used as the vehicle control.

4.2.4 Cell Lysis and Western Blotting

Cell lysis and western blot were performed as described in section 3.2.4.

4.3 Results and Discussion

4.3.1 K777 Treatment Leads to Post-Transcriptional Accumulation of MMP14

The proteomics analysis indicates a higher level of MMP14 in K777-treated neuroblastoma cells [90]. To validate the proteomics data and test whether K777 has an effect on exogenously expressed MMP14, MMP14 construct was expressed in the HEK293T cells with or without K777 treatment. As shown in Fig. 10, compared to control cells, a much higher level of MMP14 was observed in K777-treated cells, suggesting that K777 treatment leads to post–transcriptional accumulation of MMP14, and that this effect of K777 on MMP14 is independent of cell line. However, since the molecular weight difference between the pro- and active form of MMP14 is only around 2 KD, the main form of the MMP14 accumulates in K777-treated cells is unknown. The effect of K777 treatment on ADAM10, which is a member of the ADAM metalloproteinases family, was also tested. However, due to the instability of the ADAM10 protein and potentially an unknown problem with the ADAM10 construct, the expression of ADAM10 was not detected.

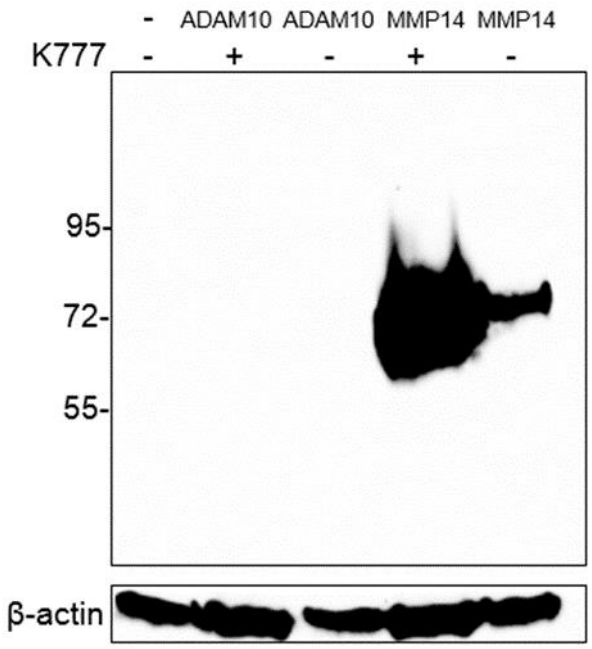

Figure 10: K777 treatment leads to post-transcriptional accumulation of MMP14. HEK293T cells were transfected with 1 μg of plasmid encoding C-terminal myc-tagged human ADAM10 or C-terminal myc_6-tagged mouse MMP14, and cultured with or without 10 μM K777 for 3 days. Cell lysates were processed for western blot with an anti-myc antibody.

4.3.2 K777 Treatment Leads to Post-Transcriptional Accumulation of PTK7

PTK7 and EphA2, which are 2 known substrates of MMP14 and were also shown to accumulate in K777-treated neuroblastoma cells by the proteomics analysis [90, 98-99], were used to detect the activity of MMP14 under K777 treatment (Fig. 11). Since mouse EphA2 construct was not available at the time this experiment was conducted, a *Xenopus* EphA2 construct was used instead and its expression was not detected. However, a higher level of PTK7 was observed in K777-treated cells compared to control cells, indicating a lower activity of MMP14 in K777-treated cells. This result, combined with the fact that a higher level of MMP14 was observed in K777-treated cells, suggests that the MMP14 accumulating in K777-treated cells is

mainly the pro-form, which has a propeptide to inhibit its protease activity and is not capable of cleaving PTK7.

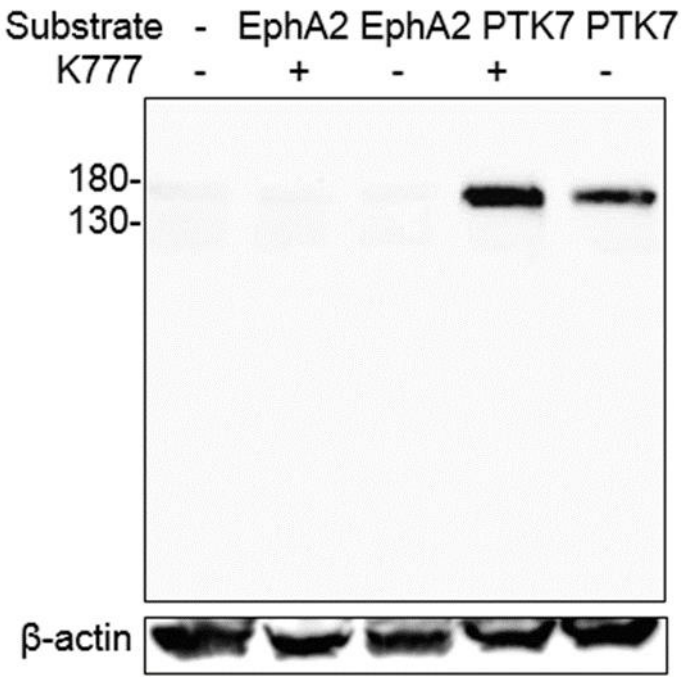

Figure 11: K777 treatment leads to post-transcriptional accumulation of PTK7. HEK293T cells were transfected with 1 μg of plasmid encoding C-terminal HA-tagged *Xenopus* EphA2 or mouse PTK7, and cultured with or without 10 μM K777 for 2 days. Cell lysates were processed for western blot with an anti-HA antibody.

4.3.3 The Effect of K777 on MMP14 Depends on MMP14 Protease Activity

Our results suggested that the MMP14 accumulates in K777-treated cells is mainly pro-form MMP14, which has a propeptide to inhibit its protease activity and is not able to cleave substrates. The active form of MMP14, on the other hand, is capable of cleaving various substrates and has been shown to degrade itself through autocleavage [96-97]. Therefore, the accumulation of MMP14 observed upon K777

treatment may be caused by less autocleavage of the MMP14 in K777-treated cells. To test this hypothesis, wild-type MMP14 (WT) and protease-dead mutant of MMP14 (E/A) were expressed in the HEK293T cells with or without K777 treatment. As expected, although higher level of wild-type MMP14 was observed in K777-treated cells compared to control cells, the level of protease-dead MMP14 remains the same in control and K777-treated cells after normalization (Fig. 12), indicating that the effect of K777 on MMP14 depends on MMP14 protease activity and the accumulation of MMP14 observed under K777 treatment may be caused by less autocleavage.

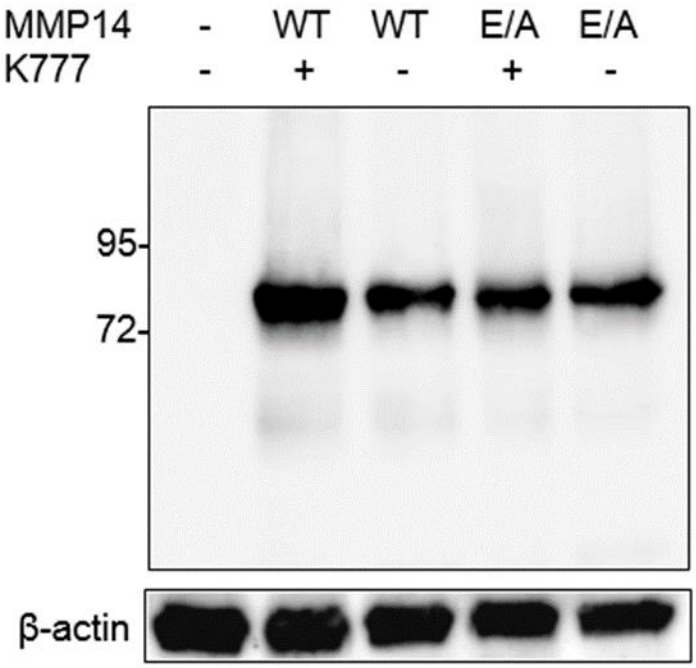

Figure 12: The effect of K777 on MMP14 depends on MMP14 protease activity. HEK293T cells were transfected with 1 μg of plasmid encoding C-terminal myc_6-tagged wild-type mouse MMP14 (WT) or a protease-dead mutant (E/A), and incubated with or without 10 μM K777 for 2 days to avoid cell death observed in 3-day treatment. Cell lysates were processed for western blot with an anti-myc antibody.

4.4 Conclusion and Future Directions

In this study, I investigated the level and activity of MMP14 under K777 treatment. I found that K777 treatment leads to accumulation of MMP14 and this effect is likely post-transcriptional and independent of cell line. I also detected the activity of MMP14 under K777 treatment by substrate cleavage assay, and a lower activity of MMP14 was found in K777-treated cells, indicating that the MMP14 accumulates under K777 treatment is mainly in its inactive pro-form. I then investigated the role of MMP14 protease activity in the process by expressing the protease-dead mutant MMP14 in the cells under K777 treatment. I found that the level of protease-dead MMP14 remains the same in control and K777-treated cells, indicating that the effect of K777 on MMP14 depends on MMP14 protease activity and the accumulation of MMP14 observed under K777 treatment may be caused by less autocleavage of the MMP14 in K777-treated cells. My findings help to delineate the molecular mechanism through which K777 regulates MMP14, and provide important insight on targeting cathepsins B and L as a novel approach to treat neuroblastoma.

Substrate cleavage assay was used to detect the activity of MMP14 under K777 treatment in this study. However, the expression of only one of the substrates of MMP14 was detected successfully. In the future, more substrates of MMP14, such as mouse EphA2 and ProMMP2 [94, 99], should be used to further confirm the activity of the MMP14 under K777 treatment. I will also try to separate the pro- and active forms of MMP14 in my western blot analyses by increasing gel running time. Finally, future research that studies the level and activity of MMP14 upon siRNA-mediated knockdown of cathepsins B and L would be helpful to further reveal the molecular

mechanism that regulates MMP14 under K777 treatment and clarify the role of cathepsins B and L in this process.

REFERENCES

1. Bode, W., Gomis-Rüth, F. X., & Stöckler, W. (1993). Astacins, serralysins, snake venom and matrix metalloproteinases exhibit identical zinc-binding environments (HEXXHXXGXXH and Met-turn) and topologies and should be grouped into a common family, the 'metzincins'. *FEBS letters*, *331*(1-2), 134-140.

2. Rivera, S., Khrestchatisky, M., Kaczmarek, L., Rosenberg, G. A., & Jaworski, D. M. (2010). Metzincin proteases and their inhibitors: foes or friends in nervous system physiology?. *Journal of Neuroscience*, *30*(46), 15337-15357.

3. Huxley-Jones, J., Clarke, T. K., Beck, C., Toubaris, G., Robertson, D. L., & Boot-Handford, R. P. (2007). The evolution of the vertebrate metzincins; insights from Ciona intestinalis and Danio rerio. *BMC evolutionary biology*, *7*(1), 63.

4. Murphy, G., & Lee, M. H. (2005). What are the roles of metalloproteinases in cartilage and bone damage?. *Annals of the rheumatic diseases*, *64*(suppl 4), iv44-iv47.

5. Escalona, R. M., Chan, E., Kannourakis, G., Findlay, J. K., & Ahmed, N. (2018). The Many Facets of Metzincins and Their Endogenous Inhibitors: Perspectives on Ovarian Cancer Progression. *International journal of molecular sciences*, *19*(2), 450.

6. Khalid, A., & Javaid, M. A. (2016). Matrix Metalloproteinases: New Targets in Cancer Therapy. *J Cancer Sci Ther*, *8*, 143-153.

7. Duffy, M. J., Mullooly, M., O'Donovan, N., Sukor, S., Crown, J., Pierce, A., & McGowan, P. M. (2011). The ADAMs family of proteases: new biomarkers and therapeutic targets for cancer?. *Clinical proteomics*, *8*(1), 9.

8. Seals, D. F., & Courtneidge, S. A. (2003). The ADAMs family of metalloproteases: multidomain proteins with multiple functions. *Genes & development*, *17*(1), 7-30.

9. Wong, E., Maretzky, T., Peleg, Y., Blobel, C., & Sagi, I. (2015). The Functional Maturation of A Disintegrin and Metalloproteinase (ADAM) 9, 10 and 17 Requires Processing at a Newly Identified Proprotein Convertase (PC) Cleavage Site. *Journal of Biological Chemistry*, jbc-M114.

10. Blobel, C. P. (2005). ADAMs: key components in EGFR signalling and development. *Nature reviews Molecular cell biology*, *6*(1), 32.

11. Verma, R. P., & Hansch, C. (2007). Matrix metalloproteinases (MMPs): chemical–biological functions and (Q) SARs. *Bioorganic & medicinal chemistry*, *15*(6), 2223-2268.

12. Christian, L., Bahudhanapati, H., & Wei, S. (2013). Extracellular metalloproteinases in neural crest development and craniofacial morphogenesis. *Critical reviews in biochemistry and molecular biology*, *48*(6), 544-560.

13. Remacle, A. G., Rozanov, D. V., Fugere, M., Day, R., & Strongin, A. Y. (2006). Furin regulates the intracellular activation and the uptake rate of cell surface-associated MT1-MMP. *Oncogene*, *25*(41), 5648.

14. Steenport, M., Khan, K. F., Du, B., Barnhard, S. E., Dannenberg, A. J., & Falcone, D. J. (2009). Matrix metalloproteinase (MMP)-1 and MMP-3 induce macrophage MMP-9: evidence for the role of TNF-α and cyclooxygenase-2. *The Journal of Immunology*, *183*(12), 8119-8127.

15. Itoh, Y. (2015). Membrane-type matrix metalloproteinases: Their functions and regulations. *Matrix Biology*, *44*, 207-223.

16. Sato, H., Takino, T., Okada, Y., Cao, J., Shinagawa, A., Yamamoto, E., & Seiki, M. (1994). A matrix metalloproteinase expressed on the surface of invasive tumour cells. *Nature*, *370*(6484), 61.

17. Yan, T., Lin, Z., Jiang, J., Lu, S., Chen, M., Que, H., ... & Zheng, Q. (2015). MMP14 regulates cell migration and invasion through epithelial-mesenchymal transition in nasopharyngeal carcinoma. *American journal of translational research*, *7*(5), 950.

18. Ip, Y. C., Cheung, S. T., & Fan, S. T. (2004). MMP14 enhances tumour growth and invasion in hepatocellular carcinoma.

19. Kobayashi, K., Nishioka, M., Kohno, T., Nakamoto, M., Maeshima, A., Aoyagi, K., ... & Yokota, J. (2004). Identification of genes whose expression is upregulated in lung adenocarcinoma cells in comparison with type II alveolar cells and bronchiolar epithelial cells in vivo. *Oncogene*, *23*(17), 3089.

20. Benson, C. S., Babu, S. D., Radhakrishna, S., Selvamurugan, N., & Sankar, B. R. (2013). Expression of matrix metalloproteinases in human breast cancer tissues. *Disease markers*, *34*(6), 395-405.

21. Shen, Z., Wang, X., Yu, X., Zhang, Y., & Qin, L. (2017). MMP16 promotes tumor metastasis and indicates poor prognosis in hepatocellular carcinoma. *Oncotarget*, *8*(42), 72197.

22. Siegel, R. L., Miller, K. D., Fedewa, S. A., Ahnen, D. J., Meester, R. G., Barzi, A., & Jemal, A. (2017). Colorectal cancer statistics, 2017. *CA: a cancer journal for clinicians*, 67(3), 177-193.

23. Stewart, B. W. K. P., & Wild, C. P. (2017). World cancer report 2014. *Health*.

24. Markowitz, S. D., & Bertagnolli, M. M. (2009). Molecular basis of colorectal cancer. *New England Journal of Medicine*, 361(25), 2449-2460.

25. Siegel, R. L., Miller, K. D., & Jemal, A. (2016). Cancer statistics, 2016. *CA: a cancer journal for clinicians*, *66*(1), 7-30.

26. Ionov, Y., Peinado, M. A., Malkhosyan, S., Shibata, D., & Perucho, M. (1993). Ubiquitous somatic mutations in simple repeated sequences reveal a new mechanism for colonic carcinogenesis. *Nature*, 363(6429), 558.

27. Khalek, F. J. A., Gallicano, G. I., & Mishra, L. (2010). Colon cancer stem cells. *Gastrointestinal cancer research: GCR*, (Suppl 1), S16.

28. Goessling, W., North, T. E., Loewer, S., Lord, A. M., Lee, S., Stoick-Cooper, C. L., ... & Zon, L. I. (2009). Genetic interaction of PGE2 and Wnt signaling regulates developmental specification of stem cells and regeneration. *Cell*, 136(6), 1136-1147.

29. Paul, I., Bhattacharya, S., Chatterjee, A., & Ghosh, M. K. (2013). Current understanding on EGFR and Wnt/β-catenin signaling in glioma and their possible crosstalk. *Genes & cancer*, 4(11-12), 427-446.

30. Giebeler, N., & Zigrino, P. (2016). A disintegrin and metalloprotease (ADAM): Historical overview of their functions. *Toxins*, 8(4), 122.

31. Duffy, M. J., McKiernan, E., O'Donovan, N., & McGowan, P. M. (2009). Role of ADAMs in cancer formation and progression. *Clinical Cancer Research*, 15(4), 1140-1144.

32. Peduto, L. (2009). ADAM9 as a potential target molecule in cancer. *Current pharmaceutical design*, 15(20), 2282-2287.

33. Perfetto, M. (2017). ADAM9 silencing inhibits colorectal tumor cell migration in vitro. Unpublished manuscript.

34. Andrews, S. (2010). FastQC: a quality control tool for high throughput sequence data.

35. Krueger, F. (2015). Trim galore. A wrapper tool around Cutadapt and FastQC to consistently apply quality and adapter trimming to FastQ files.

36. Kim, D., Pertea, G., Trapnell, C., Pimentel, H., Kelley, R., & Salzberg, S. L. (2013). TopHat2: accurate alignment of transcriptomes in the presence of insertions, deletions and gene fusions. *Genome biology*, 14(4), R36.

37. Anders, S., Pyl, P. T., & Huber, W. (2015). HTSeq—a Python framework to work with high-throughput sequencing data. *Bioinformatics*, 31(2), 166-169.

38. Robinson, M. D., McCarthy, D. J., & Smyth, G. K. (2010). edgeR: a Bioconductor package for differential expression analysis of digital gene expression data. *Bioinformatics*, 26(1), 139-140.

39. Anders, S., & Huber, W. (2012). Differential expression of RNA-Seq data at the gene level–the DESeq package. Heidelberg, Germany: European Molecular Biology Laboratory (EMBL).

40. Kuleshov, M. V., Jones, M. R., Rouillard, A. D., Fernandez, N. F., Duan, Q., Wang, Z., ... & McDermott, M. G. (2016). Enrichr: a comprehensive gene set enrichment analysis web server 2016 update. *Nucleic acids research*, 44(W1), W90-W97.

41. Biechele, T. L., Kulikauskas, R. M., Toroni, R. A., Lucero, O. M., Swift, R. D., James, R. G., ... & Chien, A. J. (2012). Wnt/β-catenin signaling and AXIN1 regulate apoptosis triggered by inhibition of the mutant kinase BRAFV600E in human melanoma. *Sci. Signal*., 5(206), ra3-ra3.

42. Jeong, W. J., Yoon, J., Park, J. C., Lee, S. H., Lee, S. H., Kaduwal, S., ... & Choi, K. Y. (2012). Ras stabilization through aberrant activation of Wnt/β-catenin signaling promotes intestinal tumorigenesis. *Sci. Signal*., 5(219), ra30-ra30.

43. Farhan, M., Wang, H., Gaur, U., Little, P. J., Xu, J., & Zheng, W. (2017). FOXO Signaling Pathways as Therapeutic Targets in Cancer. *International journal of biological sciences*, 13(7), 815.

44. Hoogeboom, D., Essers, M. A., Polderman, P. E., Voets, E., Smits, L. M., & Boudewijn, M. T. (2008). Interaction of FOXO with β-catenin inhibits β-catenin/T cell factor activity. *Journal of Biological Chemistry*, 283(14), 9224-9230.

45. Kim, N. H., Kim, H. S., Kim, N. G., Lee, I., Choi, H. S., Li, X. Y., ... & Park, C. (2011). p53 and microRNA-34 are suppressors of canonical Wnt signaling. *Sci. Signal.*, *4*(197), ra71-ra71.

46. Bhutia, Y. D., & Ganapathy, V. (2016). Glutamine transporters in mammalian cells and their functions in physiology and cancer. *Biochimica et Biophysica Acta (BBA)-Molecular Cell Research*, 1863(10), 2531-2539.

47. Levine, A. J. (1997). p53, the cellular gatekeeper for growth and division. *cell*, 88(3), 323-331.

48. Yagami-Hiromasa, T., Sato, T., Kurisaki, T., Kamijo, K., Nabeshima, Y. I., & Fujisawa-Sehara, A. (1995). A metalloprotease-disintegrin participating in myoblast fusion. *Nature*, 377(6550), 652.

49. Hooper, N. M., & Lendeckel, U. (Eds.). (2006). The Adam family of proteases (Vol. 4). *Springer Science & Business Media*.

50. Edwards, D. R., Handsley, M. M., & Pennington, C. J. (2008). The ADAM metalloproteinases. *Molecular aspects of medicine*, 29(5), 258-289.

51. Asakura, M., Kitakaze, M., Takashima, S., Liao, Y., Ishikura, F., Yoshinaka, T., ... & Asanuma, H. (2002). Cardiac hypertrophy is inhibited by antagonism of ADAM12 processing of HB-EGF: metalloproteinase inhibitors as a new therapy. *Nature medicine*, 8(1), 35.

52. Horiuchi, K., Le Gall, S., Schulte, M., Yamaguchi, T., Reiss, K., Murphy, G., ... & Blobel, C. P. (2007). Substrate selectivity of epidermal growth factor-receptor ligand sheddases and their regulation by phorbol esters and calcium influx. *Molecular biology of the cell*, 18(1), 176-188.

53. Yarden, Y., & Sliwkowski, M. X. (2001). Untangling the ErbB signalling network. *Nature reviews Molecular cell biology*, 2(2), 127.

54. Dyczynska, E., Sun, D., Yi, H., Sehara-Fujisawa, A., Blobel, C. P., & Zolkiewska, A. (2007). Proteolytic processing of delta-like 1 by ADAM proteases. *Journal of Biological Chemistry*, 282(1), 436-444.

55. Roy, R., Wewer, U. M., Zurakowski, D., Pories, S. E., & Moses, M. A. (2004). ADAM12 cleaves extracellular matrix proteins and correlates with cancer status and stage. *Journal of Biological Chemistry*, 279(49), 51323-51330.

56. Loechel, F., Fox, J. W., Murphy, G., Albrechtsen, R., & Wewer, U. M. (2000). ADAM 12-S cleaves IGFBP-3 and IGFBP-5 and is inhibited by TIMP-3. *Biochemical and biophysical research communications*, 278(3), 511-515.

57. Shi, Z., Xu, W., Loechel, F., Wewer, U. M., & Murphy, L. J. (2000). ADAM 12, a disintegrin metalloprotease, interacts with insulin-like growth factor-binding protein-3. *Journal of Biological Chemistry*, 275(24), 18574-18580.

58. Estrella, C., Rocks, N., Paulissen, G., Quesada-Calvo, F., Noël, A., Vilain, E., ... & Gosset, P. (2009). Role of A disintegrin and metalloprotease-12 in neutrophil recruitment induced by airway epithelium. *American journal of respiratory cell and molecular biology*, 41(4), 449-458.

59. Bourd-Boittin, K., Le Pabic, H., Bonnier, D., L'Helgoualc'h, A., & Théret, N. (2008). RACK1, a New ADAM12 Interacting Protein CONTRIBUTION TO LIVER FIBROGENESIS. *Journal of Biological Chemistry*, 283(38), 26000-26009.

60. Wang, X., Chow, F. L., Oka, T., Hao, L., Lopez-Campistrous, A., Kelly, S., ... & Kassiri, Z. (2009). Matrix metalloproteinase-7 and ADAM-12 (a disintegrin and metalloproteinase-12) define a signaling axis in agonist-induced hypertension and cardiac hypertrophy. *Circulation*, 119(18), 2480-2489.

61. Wewer U.M., Albrechtsen R., Engvall E. (2005) ADAM12. In: Hooper N.M., Lendeckel U. (eds) The ADAM Family of Proteases. *Proteases in Biology and Disease*, vol 4. Springer, Boston, MA

62. Fröhlich, C., Albrechtsen, R., Dyrskjøt, L., Rudkjær, L., Ørntoft, T. F., & Wewer, U. M. (2006). Molecular profiling of ADAM12 in human bladder cancer. *Clinical Cancer Research*, 12(24), 7359-7368.

63. Le Pabic, H., Bonnier, D., Wewer, U. M., Coutand, A., Musso, O., Baffet, G., ... & Théret, N. (2003). ADAM12 in human liver cancers: TGF-β-regulated expression in stellate cells is associated with matrix remodeling. *Hepatology*, 37(5), 1056-1066.

64. Iba, K., Albrechtsen, R., Gilpin, B. J., Loechel, F., & Wewer, U. M. (1999). Cysteine-rich domain of human ADAM 12 (meltrin α) supports tumor cell adhesion. *The American journal of pathology*, 154(5), 1489-1501.

65. Rocks, N., Paulissen, G., Calvo, F. Q., Polette, M., Gueders, M., Munaut, C., ... & Cataldo, D. (2006). Expression of a disintegrin and metalloprotease (ADAM and ADAMTS) enzymes in human non-small-cell lung carcinomas (NSCLC). *British journal of cancer*, 94(5), 724.

66. Kodama, T., Ikeda, E., Okada, A., Ohtsuka, T., Shimoda, M., Shiomi, T., ... & Okada, Y. (2004). ADAM12 is selectively overexpressed in human glioblastomas and is associated with glioblastoma cell proliferation and shedding of heparin-binding epidermal growth factor. *The American journal of pathology*, 165(5), 1743-1753.

67. Li, J., Perfetto, M., Neuner, R., Bahudhanapati, H., Christian, L., Mathavan, K., ... & Wei, S. (2018). Xenopus ADAM19 regulates Wnt signaling and neural crest specification by stabilizing ADAM13. *Development*, 145(7), dev158154.

68. Li, A., Gao, X., Ren, J., Jin, C., & Xue, Y. (2009). BDM-PUB: computational prediction of protein ubiquitination sites with a Bayesian discriminant method. BDM-PUB: Computational Prediction of Protein Ubiquitination Sites with a Bayesian Discriminant Method.

69. Maris, J. M. (2010). Recent advances in neuroblastoma. *New England Journal of Medicine*, *362*(23), 2202-2211.

70. US Cancer Statistics Working Group. (2010). United States cancer statistics: 1999-2006 incidence and mortality Web-based report. *Atlanta: US Department of Health and Human Services, Centers for Disease Control and Prevention and National Cancer Institute*.

71. Louis, C. U., & Shohet, J. M. (2015). Neuroblastoma: molecular pathogenesis and therapy. *Annual review of medicine*, *66*, 49-63.

72. Brodeur, G. M. (2003). Neuroblastoma: biological insights into a clinical enigma. *Nature Reviews Cancer*, *3*(3), 203.

73. Tonini, G. P., & Pistoia, V. (2006). Molecularly guided therapy of neuroblastoma: a review of different approaches. *Current pharmaceutical design*, *12*(18), 2303-2317.

74. Matthay, K. K., Villablanca, J. G., Seeger, R. C., Stram, D. O., Harris, R. E., Ramsay, N. K., ... & Gerbing, R. B. (1999). Treatment of high-risk neuroblastoma with intensive chemotherapy, radiotherapy, autologous bone marrow transplantation, and 13-cis-retinoic acid. *New England Journal of Medicine*, *341*(16), 1165-1173.

75. Conus, S., & Simon, H. U. (2010). Cathepsins and their involvement in immune responses. *Swiss Med Wkly*, *140*, w13042.

76. Turk, V., Turk, B., & Turk, D. (2001). Lysosomal cysteine proteases: facts and opportunities. *The EMBO journal*, *20*(17), 4629-4633.

77. Zavašnik-Bergant, T., & Turk, B. (2006). Cysteine cathepsins in the immune response. *HLA*, *67*(5), 349-355.

78. Vasiljeva, O., Reinheckel, T., Peters, C., Turk, D., Turk, V., & Turk, B. (2007). Emerging roles of cysteine cathepsins in disease and their potential as drug targets. *Current pharmaceutical design*, *13*(4), 387-403.

79. Nomura, T., & Katunuma, N. (2005). Involvement of cathepsins in the invasion, metastasis and proliferation of cancer cells. *The journal of medical investigation*, *52*(1, 2), 1-9.

80. Levičar, N., Kos, J., Blejec, A., Golouh, R., Vrhovec, I., Frkovič-Grazio, S., & Lah, T. T. (2002). Comparison of potential biological markers cathepsin B, cathepsin L, stefin A and stefin B with urokinase and plasminogen activator inhibitor-1 and clinicopathological data of breast carcinoma patients. *Cancer detection and prevention*, *26*(1), 42-49.

81. Friedrich, B., Jung, K., Lein, M., Türk, I., Rudolph, B., Hampel, G., ... & Loening, S. A. (1999). Cathepsins B, H, L and cysteine protease inhibitors in malignant prostate cell lines, primary cultured prostatic cells and prostatic tissue. *European Journal of Cancer*, *35*(1), 138-144.

82. Foekens, J. A., Kos, J., Peters, H. A., Krasovec, M., Look, M. P., Cimerman, N., ... & Klijn, J. G. (1998). Prognostic significance of cathepsins B and L in primary human breast cancer. *Journal of clinical oncology*, *16*(3), 1013-1021.

83. Strojnik, T., idanik, B., Kos, J., & Lah, T. T. (2001). Cathepsins B and L are markers for clinically invasive types of meningiomas. *Neurosurgery*, *48*(3), 598-605.

84. Pucer, A., Castino, R., Mirković, B., Falnoga, I., Šlejkovec, Z., Isidoro, C., & Lah, T. T. (2010). Differential role of cathepsins B and L in autophagy-associated cell death induced by arsenic trioxide in U87 human glioblastoma cells. *Biological chemistry*, *391*(5), 519-531.

85. Rempel, S. A., Rosenblum, M. L., Mikkelsen, T., Yan, P. S., Ellis, K. D., Golembieski, W. A., ... & Sloane, B. F. (1994). Cathepsin B expression and localization in glioma progression and invasion. *Cancer research*, *54*(23), 6027-6031.

86. Jacobsen, W., Christians, U., & Benet, L. Z. (2000). In vitro evaluation of the disposition of a novel cysteine protease inhibitor. *Drug metabolism and disposition*, *28*(11), 1343-1351.

87. Engel, J. C., Doyle, P. S., Hsieh, I., & McKerrow, J. H. (1998). Cysteine protease inhibitors cure an experimental Trypanosoma cruzi infection. *Journal of Experimental Medicine*, *188*(4), 725-734.

88. Doyle, P. S., Zhou, Y. M., Engel, J. C., & McKerrow, J. H. (2007). A cysteine protease inhibitor cures Chagas' disease in an immunodeficient-mouse model of infection. *Antimicrobial agents and chemotherapy*, *51*(11), 3932-3939.

89. Barr, S. C., Warner, K. L., Kornreic, B. G., Piscitelli, J., Wolfe, A., Benet, L., & McKerrow, J. H. (2005). A cysteine protease inhibitor protects dogs from cardiac damage during infection by Trypanosoma cruzi. *Antimicrobial agents and chemotherapy*, *49*(12), 5160-5161.

90. Halakos. E. (2018). K11777 induce autophagy and cell death in neuroblastoma cells. Unpublished manuscript.

91. Snyman, C., & Niesler, C. U. (2015). MMP-14 in skeletal muscle repair. *Journal of muscle research and cell motility*, *36*(3), 215-225.

92. Nakada, M., Nakamura, H., Ikeda, E., Fujimoto, N., Yamashita, J., Sato, H., ... & Okada, Y. (1999). Expression and tissue localization of membrane-type 1, 2, and 3 matrix metalloproteinases in human astrocytic tumors. *The American journal of pathology*, *154*(2), 417-428.

93. Kuscu, C., Evensen, N., & Cao, J. (2011). MMP14 (matrix metallopeptidase 14 (membrane-inserted)).

94. Nishida, Y., Miyamori, H., Thompson, E. W., Takino, T., Endo, Y., & Sato, H. (2008). Activation of matrix metalloproteinase-2 (MMP-2) by membrane type 1 matrix metalloproteinase through an artificial receptor for proMMP-2 generates active MMP-2. *Cancer research*, *68*(21), 9096-9104.

95. Itoh, Y., & Seiki, M. (2006). MT1-MMP: a potent modifier of pericellular microenvironment. *Journal of cellular physiology*, *206*(1), 1-8.

96. Remacle, A. G., Chekanov, A. V., Golubkov, V. S., Savinov, A. Y., Rozanov, D. V., & Strongin, A. Y. (2006). O-glycosylation regulates autolysis of cellular membrane type-1 matrix metalloproteinase (MT1-MMP). *Journal of Biological Chemistry*, *281*(25), 16897-16905.

97. Rozanov, D. V., & Strongin, A. Y. (2003). Membrane type-1 matrix metalloproteinase functions as a proprotein self-convertase Expression of the latent zymogen in Pichia pastoris, autolytic activation, and the peptide sequence of the cleavage forms. *Journal of Biological Chemistry*, *278*(10), 8257-8260.

98. Golubkov, V. S., Chekanov, A. V., Cieplak, P., Aleshin, A. E., Chernov, A. V., Zhu, W., ... & Strongin, A. Y. (2010). The Wnt/planar cell polarity (PCP) protein tyrosine kinase-7 (PTK7) is a highly efficient proteolytic target of membrane type-1 matrix metalloproteinase (MT1-MMP): implications in cancer and embryogenesis. *Journal of Biological Chemistry*, jbc-M110.

99. Sugiyama, N., Gucciardo, E., Tatti, O., Varjosalo, M., Hyytiäinen, M., Gstaiger, M., & Lehti, K. (2013). EphA2 cleavage by MT1-MMP triggers single cancer cell invasion via homotypic cell repulsion. *J Cell Biol*, *201*(3), 467-484.